

Article

# Anti-Freezing, Non-Drying, Localized Stiffening, and Shape-Morphing Organohydrogels

Jiayan Shen <sup>1</sup>, Shutong Du <sup>1</sup>, Ziyao Xu <sup>1</sup>, Tiansheng Gan <sup>1</sup>, Stephan Handschuh-Wang <sup>1</sup> and Xueli Zhang <sup>1,\*</sup>

<sup>1</sup> College of Chemistry and Environmental Engineering, Shenzhen University, Shenzhen, China; 2170225620@email.szu.edu.cn (J.S.); 2060221013@email.szu.edu.cn (S.D.); 1910223058@email.szu.edu.cn (Z.X.); gantiansheng@szu.edu.cn (T.G.); stephan@szu.edu.cn (S.H.-W.);

\* Correspondence: xlzhang@szu.edu.cn; Tel.: +86-755-26557377

## Supporting Information

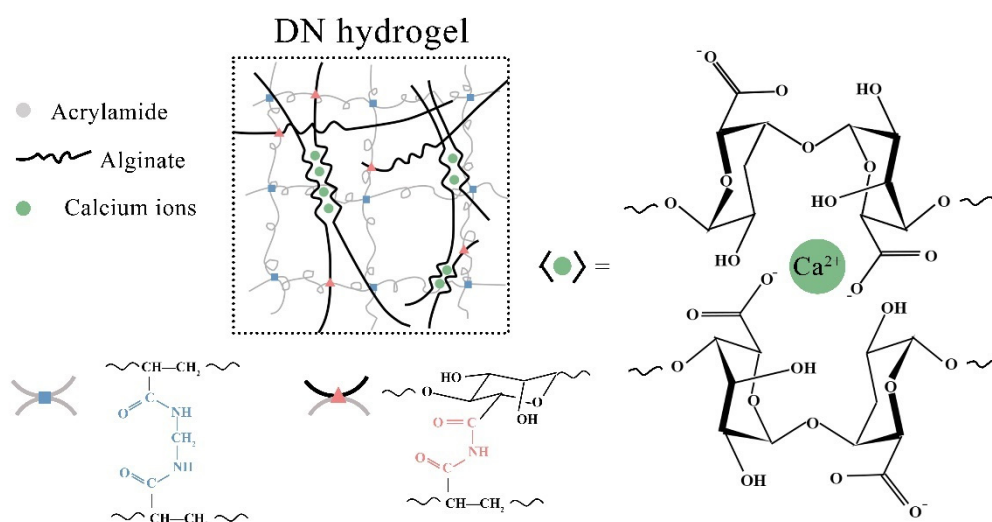


**Figure S1.** Schematic illustration of the double network (DN) hydrogel (top left) and its corresponding constituents alginate gel (crosslinked by  $\text{Ca}^{2+}$ , right) and crosslinked polyacrylamide (bottom left, blue). Furthermore, the crosslink between the polyacrylamide and alginate gel is illustrated (bottom middle).

The FTIR spectra of the three gels (DN hydrogel, glycerol-based organohydrogel, and stiffened gel) are shown in Figure S2. The alginate in the DN gel exhibits a broad peak near  $3340\text{ cm}^{-1}$ , indicative for O–H stretching, a sharp peak at  $1600\text{ cm}^{-1}$  assigned to asymmetric  $\text{COO}^-$  stretching, and two peaks at  $1420$  and  $1320\text{ cm}^{-1}$  for C–H deformation with secondary alcohols. Furthermore, three peaks at  $1120$ ,  $1090$ , and  $1030\text{ cm}^{-1}$  were found for asymmetric C–O–C stretching, C–O stretching in CH–OH structure, and symmetric C–O stretching in C–O–C structure, respectively. Similarly, in the hydrogel, the bands for polyacrylamide were found. The gel exhibited bands at  $3360\text{ cm}^{-1}$  and  $3200\text{ cm}^{-1}$ , which correspond to a stretching vibration of N–H. The band at  $1660\text{ cm}^{-1}$  is indicative for C=O stretching. The bands at  $1600\text{ cm}^{-1}$  (N–H deformation for primary amine),  $1450\text{ cm}^{-1}$  ( $\text{CH}_2$  in-plane scissoring, very minor),  $1420\text{ cm}^{-1}$  (C–N stretching for primary amide),  $1350\text{ cm}^{-1}$  (C–H deformation), and  $1120\text{ cm}^{-1}$  ( $\text{NH}_2$  in-plane rocking) were also detected. The spectrum of the DN gel features a peak at  $1280\text{ cm}^{-1}$  for C–N stretching of secondary amide, which was formed during polymerization. This result indicates chemical bond formation between  $-\text{NH}_2$  groups of polyacrylamide and carboxyl groups of alginate.

The organohydrogel features similar absorption bands to the DN hydrogel. In addition, it features the bands stemming from the glycerol, and due to the presence of an abundance of glycerol in the gel, these bands are stronger than that of the gel. Novel bands are as follows. The band at  $850\text{ cm}^{-1}$  denotes C–C rocking, the band at  $920\text{ cm}^{-1}$  denotes C–OH stretching, and the band at  $1100\text{ cm}^{-1}$  denotes the C–O stretching vibration. Further new bands are at  $1200\text{ cm}^{-1}$  (C–H wagging),  $1450\text{ cm}^{-1}$  (C–H bending), and  $2875\text{ cm}^{-1}$  (symmetric C–H stretching). [54] Slight shifts in band location ( $10\text{ cm}^{-1}$ ) might be due to association effects, i.e., association with glycerol or ions. [55] We assume that the reduction in absorption band at  $1670\text{ cm}^{-1}$  is related to the association of the iron (III) with the O of the C=O.

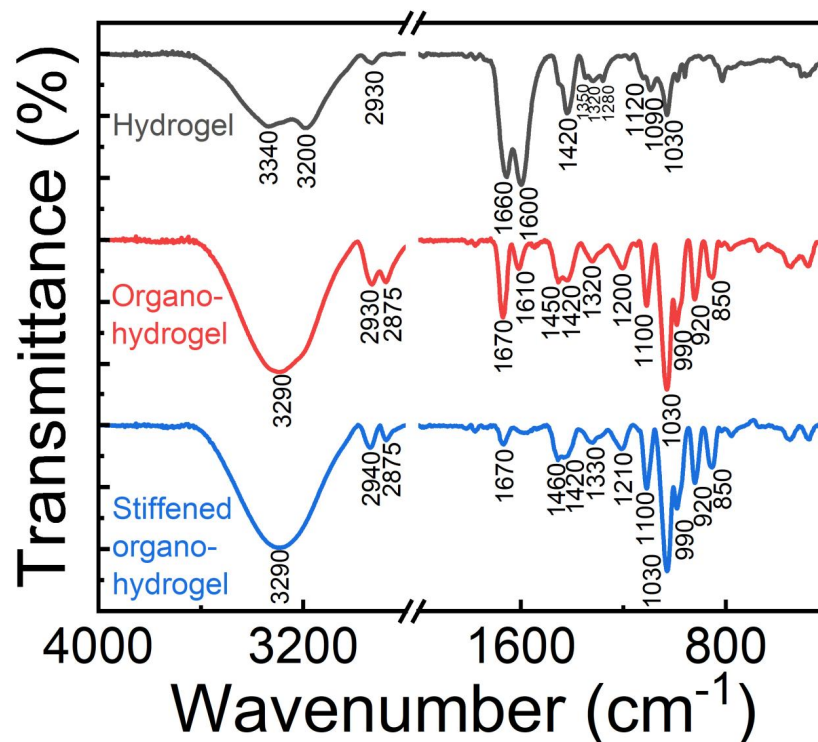


**Figure S2.** ATR-FTIR (attenuated total reflection–Fourier transform infrared) spectra of the original DN hydrogel (Ca-alginate/polyacrylamide), the glycerol-treated gel (denoted organohydrogel), and the iron (III)-treated organohydrogel (denoted stiffened organohydrogel).

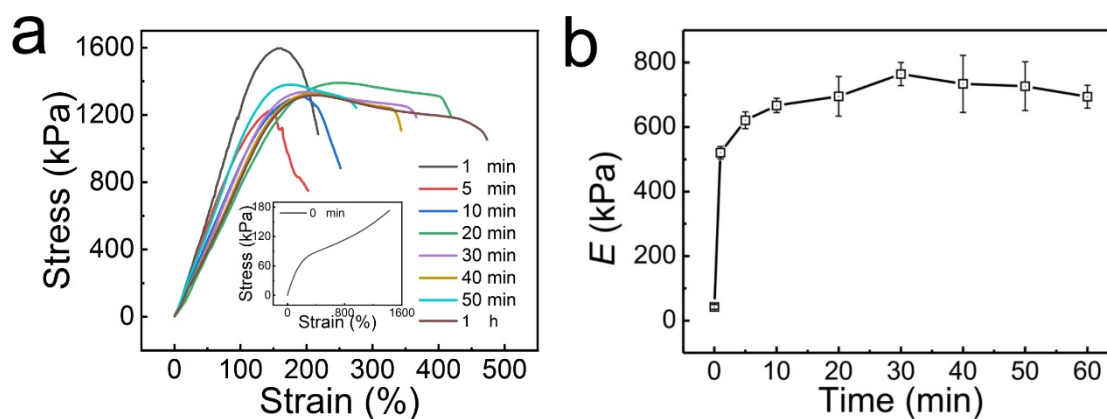


**Figure S3.** (a) The stress–strain curves and (b) the elastic modulus of the Fe(III)-stiffened Ca-alginate/PAAm organohydrogels prepared with soaking times ranging from 0 to 60 min.

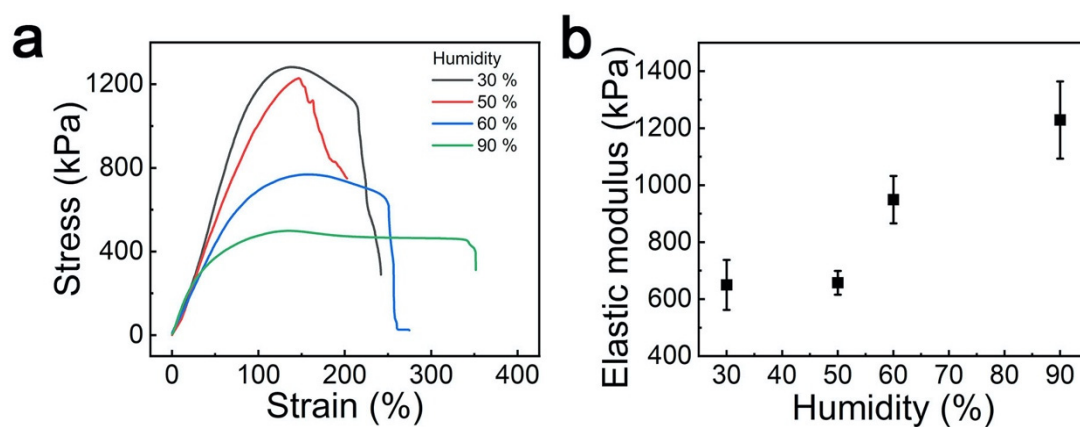


**Figure S4.** (a) Stress–strain curves of the  $\text{Fe}^{3+}$ -treated (soaking time 5 min) organohydrogel dependent on the environmental humidity. Prior to measurement, the treated organohydrogel was exposed to the environment with designated humidity for 24 h (in a humidity chamber). The test was conducted at room temperature at a speed of 20 mm/min. (b) Elastic modulus of the iron (III)-treated organohydrogel exposed to varying humidity, corresponding to the graph shown in (a).

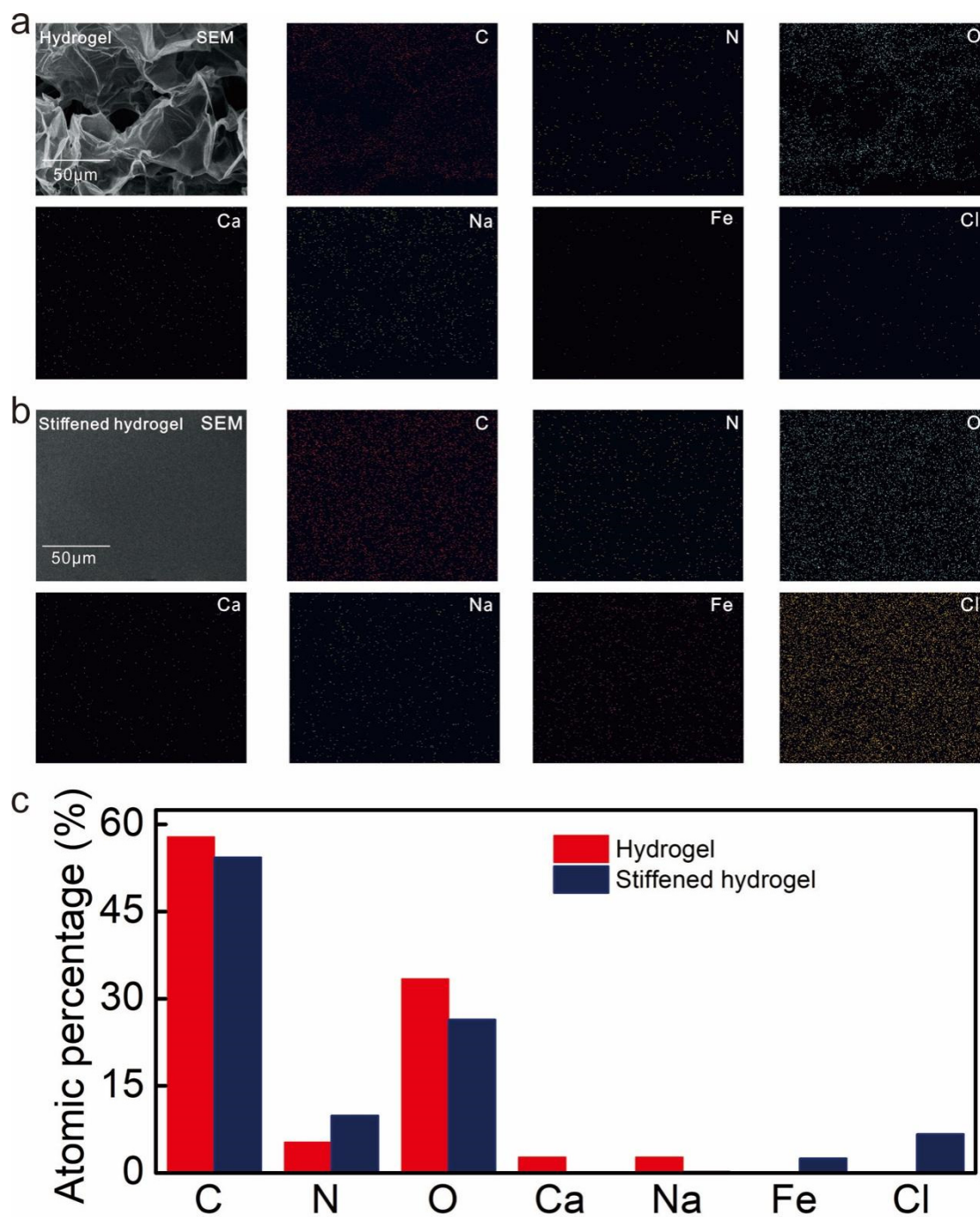


**Figure S5.** (a) SEM micrographs of the DN hydrogel and the stiffened hydrogel together with the two-dimensional energy dispersive X-ray spectroscopy (EDS) maps showing the elemental distribution of C, N, O, Ca, Na, Fe, and Cl in the gels. (b) Column diagram signifying the atomic percentage of the aforementioned elements in the hydrogel and stiffened hydrogel.

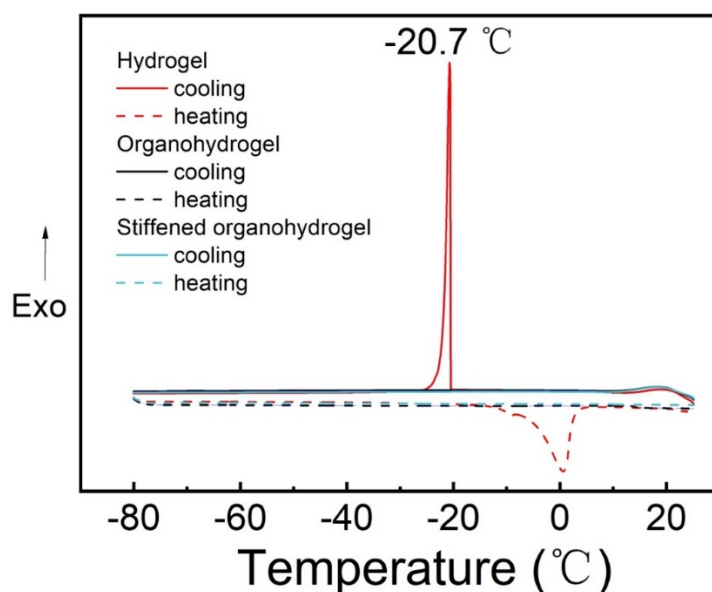


**Figure S6.** DSC thermogram of the DN hydrogel (red), organohydrogel (black), and Fe<sup>3+</sup>-treated organohydrogel in the range from  $-80$  to  $25$  °C at a heating rate of  $5$  °C/min. The solid line denotes the cooling run, while the dashed line denotes the heating run.

The thermogravimetric analysis of the hydrogel shows 3 derivatives (steps). The first at around  $100$  °C is related to the evaporation of free water. We assign the second step at around  $200$  °C to evaporation of bound water (bound by the polymer). The last step is attributed to the decomposition of the polymers ( $300$ – $400$  °C). For the organohydrogel, less water evaporates at  $100$  °C due to thorough displacement of water by glycerol. At  $200$  °C, a high weight loss is observed due to evaporation of glycerol. Decomposition of the polymer is observed at  $300$ – $400$  °C. A similar shape of the thermogram is seen for the stiffened organohydrogel. However, the water evaporation step is bigger due to the treatment with aqueous iron (III) solution.

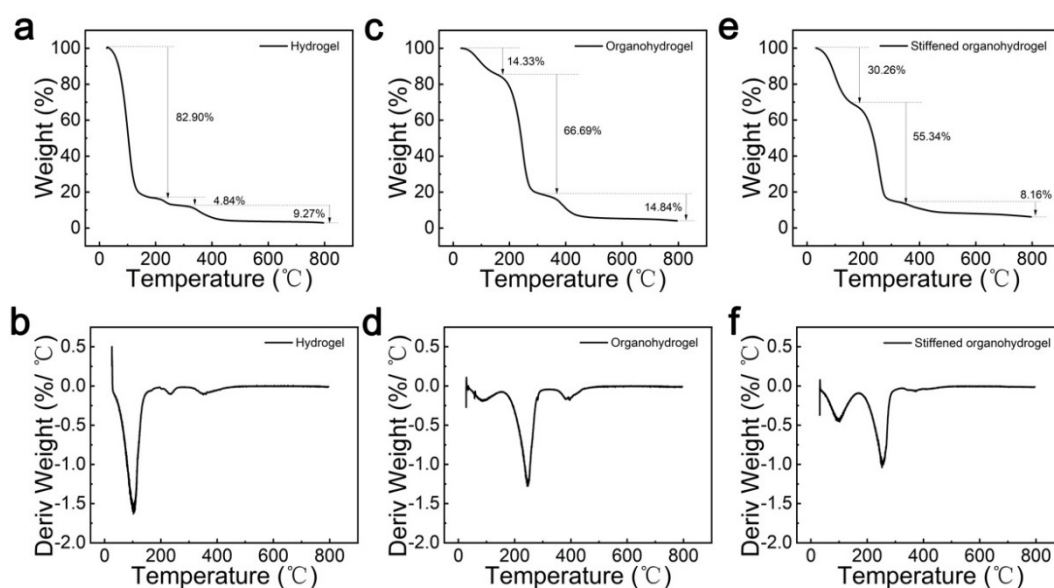


**Figure S7.** Thermogravimetric analysis (TGA) of (a) the DN hydrogel, (c) the corresponding organohydrogel, (e) and the Fe<sup>3+</sup>-treated organohydrogel in the range from room temperature up to  $800$  °C at a heating rate of  $10$  °C/min. Below each measurement, the derivative gravimetric curve is depicted: (b) DN hydrogel, (d) organohydrogel, and (f) stiffened organohydrogel.

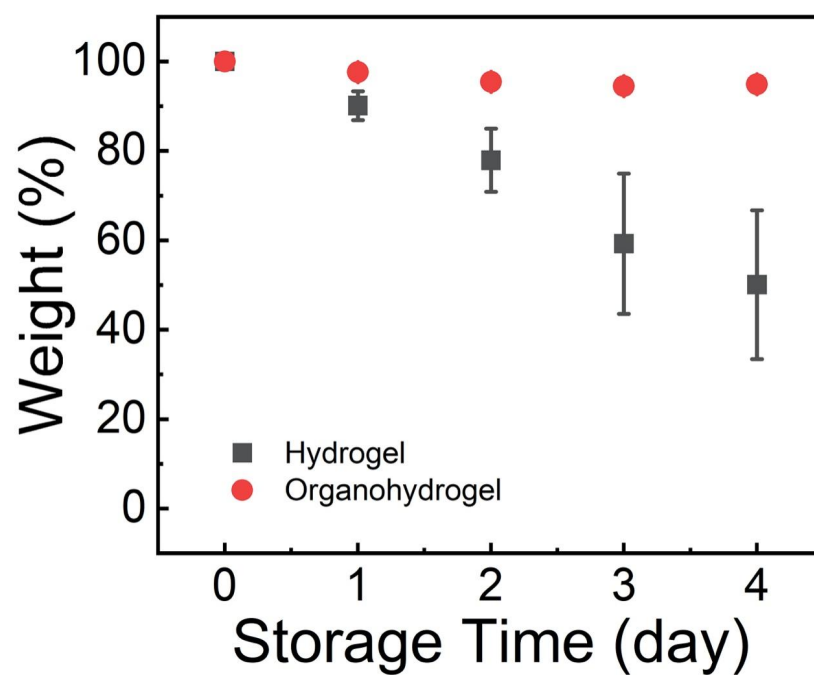


**Figure S8.** Weight retention of the organohydrogel and hydrogel upon storage in a desiccator at room temperature and 10% relative humidity.

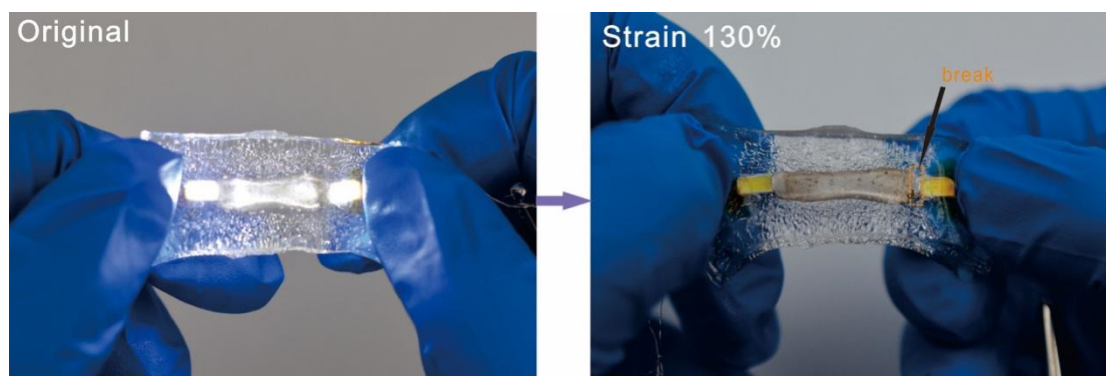


**Figure S9.** Demonstration of crack formation occurring for stiff electronics packaged in the soft organohydrogel. Upon straining the composite with a tensile strain of 130 %, a tear of the stiff conductor was observed.

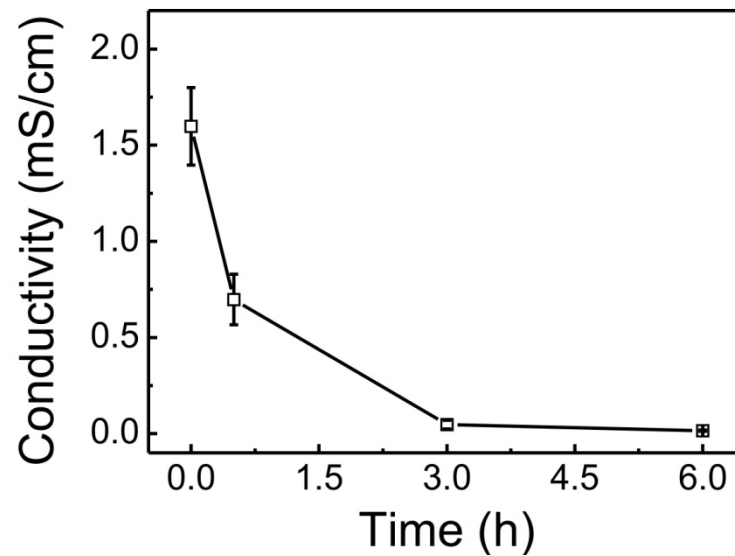


**Figure S10.** The conductivity of the hydrogel and organohydrogel prepared at different solvent displacement times from 0.5 to 6.0 h.

**Video S1:** A tough hydrogel and tough organohydrogel were cooled to a temperature of approximately  $-50$  °C. The tough hydrogel freezes quickly, while the tough organohydrogel remains unfrozen. After relaxing of a pre-applied tensile strain, the frozen tough hydrogels retains its elongated state. In contrast, the tough organohydrogel quickly folds into a 3D structure. Furthermore, we show that the folding of the tough organohydrogel is reversible by repeating the stretching–relaxing cycle.

**Video S2:** The video shows that “island–bridge” stretchable electronics can be stretched up to 1000% and that the tensile strain can be cycled for many times.